P3H-24-057, TTP24-025

PROCEEDINGS OF SCIENCE

Top-quark loops in $gg \to ZZ$ at NLO in QCD

Marco Vitti[a,b,*]

[a] *Institut für Theoretische Teilchenphysik, Karlsruhe Institute of Technology (KIT), Wolfgang-Gaede Straße 1, 76128 Karlsruhe, Germany*

[b] *Institut für Astroteilchenphysik, Karlsruhe Institute of Technology (KIT), Hermann-von-Helmholtz-Platz 1, 76344 Eggenstein-Leopoldshafen, Germany, Germany*

E-mail: marco.vitti@kit.edu

We present the calculation of the virtual corrections to $gg \to ZZ$ at next-to-leading order in QCD, focusing on the contribution from top quarks, which lacks a full analytic evaluation. The two-loop box diagrams are computed using a small-tansverse-momentum expansion, and the results are merged with those available in the high-energy expansion, in order to obtain an analytic description in the complete phase space.

Loops and Legs in Quantum Field Theory (LL2024)
14-19, April, 2024
Wittenberg, Germany

[*] Speaker

PoS(LL2024)040

1. Introduction

The production of a pair of Z bosons plays a key role in the Higgs physics program of the LHC, as well as in other tests of the Electroweak (EW) theory, and an improvement of the theoretical predictions within the Standard Model is very important in view of the High-Luminosity phase of the LHC.

Concerning the status of fixed-order predictions, the dominant partonic channel $q\bar{q} \to ZZ$ [1] is known up to next-to-next-to-leading order (NNLO) QCD [2–7] and NLO EW [8–10]. The gluon-induced channel [11, 12] is known with lower precision, and in particular the virtual NLO QCD corrections have not been computed in exact analytic form. The major challenge is in the calculation of the two-loop box diagrams that feature loops of top quarks, like the ones showed in fig. 1 (d-f). At present, these diagrams have been computed using numerical approaches [13–15] or analytic approximations [16–20]. The top loops are especially important in the region of high invariant mass of the Z-boson pair, as they give the dominant contribution to the interference between Higgs-mediated and *continuum* $gg \to ZZ$.

In these proceedings we consider the process $gg \to ZZ$ and we discuss some details of the calculation of the top-mediated box diagrams at NLO in QCD via another analytic approximation, known as the p_T expansion, which is suitable for a significant part of the phase space. This method [21, 22] relies on the expansion of the amplitude in the limit of a small transverse momentum of the final-state particles, p_T. We also discuss, following ref. [23], how this expansion can be merged with the so-called high-energy (HE) expansion [20], in order to obtain an accurate and flexible approximation over the complete phase space.

2. The $gg \to ZZ$ amplitude in the p_T expansion

We define the amplitude as

$$\mathcal{A} = \sqrt{2} m_Z^2 G_F \, \frac{\alpha_s(\mu_R)}{\pi} \delta_{ab} \, \epsilon_\mu^a(p_1) \epsilon_\nu^b(p_2) \epsilon_\rho^*(p_3) \epsilon_\sigma^*(p_4) \, \hat{\mathcal{A}}^{\mu\nu\rho\sigma}(p_1, p_2, p_3), \tag{1}$$

where G_F is the Fermi constant, $\alpha_s(\mu_R)$ is the strong coupling constant evaluated at a renormalisation scale μ_R and the polarization vectors of the gluons and the Z bosons are $\epsilon_\mu^a(p_1), \epsilon_\nu^b(p_2)$ and $\epsilon_\rho(p_3), \epsilon_\sigma(p_4)$, respectively. The Lorentz structure of the amplitude is encoded in the tensor $\hat{\mathcal{A}}^{\mu\nu\rho\sigma}(p_1, p_2, p_3)$. In order to simplify the evaluation of the cross section, we express the latter in terms of a set of 20 orthonormal projectors

$$\hat{\mathcal{A}}^{\mu\nu\rho\sigma}(p_1, p_2, p_3) = \sum_{i=1}^{20} \mathcal{P}_i^{\mu\nu\rho\sigma} \mathcal{A}_i(\hat{s}, \hat{t}, \hat{u}, m_t, m_Z, m_H), \tag{2}$$

where $\hat{s}, \hat{t}, \hat{u}$ are the partonic Mandelstam variables and m_t, m_Z, m_H are the top, Z and Higgs masses, respectively. The above decomposition relies on a specific gauge choice for the external gluons, as discussed also in refs. [20, 24, 25]. We consider a perturbative expansion of the form factors in the strong coupling

$$\mathcal{A}_i = \mathcal{A}_i^{(0)} + \frac{\alpha_s}{\pi} \mathcal{A}_i^{(1)} + O(\alpha_s^2). \tag{3}$$

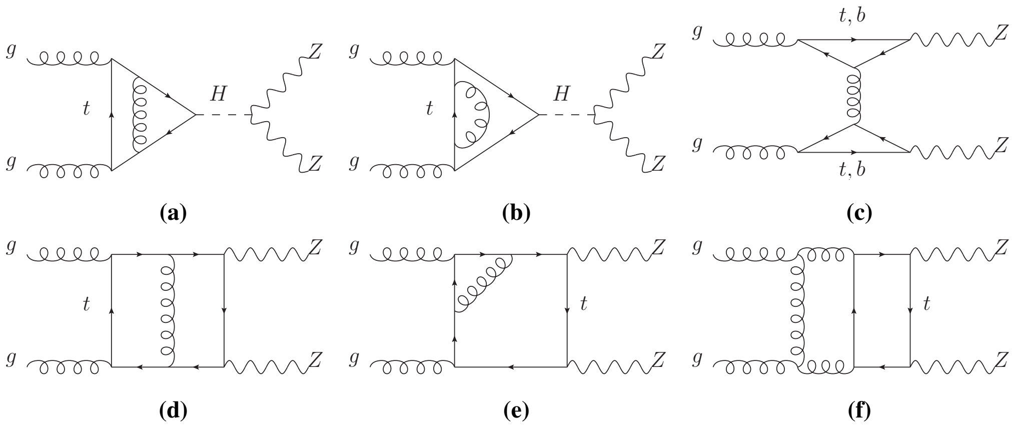

Figure 1: Representative Feynman diagrams contributing to the $gg \to ZZ$ amplitude at NLO. Loops of bottom quarks are included only in the double-triangle diagrams (c).

We are interested in the NLO form factors, which admit a decomposition in terms of diagram topologies: triangles, boxes and double triangles

$$\mathcal{A}_i^{(1)} = \mathcal{A}_i^{(1,\triangle)} + \mathcal{A}_i^{(1,\square)} + \mathcal{A}_i^{(1,\bowtie)}, \tag{4}$$

with example diagrams in fig. 1 (a,b), (d-f) and (c), respectively. Here, we discuss the calculation of the $\mathcal{A}_i^{(1,\square)}$, which is the most complicated part, as the associated Feynman integrals depend on the four energy scales $\hat{s}, \hat{t}, m_t^2, m_Z^2$.

In the p_T expansion, the $\mathcal{A}_i^{(1,\square)}$ are expanded in the limit of a forward kinematics. This is achieved by considering the *reduced* variable

$$t' = \frac{\hat{t} - m_Z^2}{2} = -\frac{s'}{2}\left\{1 - \sqrt{1 - 2\frac{p_T^2 + m_Z^2}{s'}}\right\}, \tag{5}$$

where $s' = \hat{s}/2$, and by performing an expansion of the amplitude for $t' \to 0$, which in turn is implemented via a Taylor expansion for small p_T^2 and m_Z^2. More details can be found in ref. [26]. Notably, the expansion is performed at the level of the loop *integrands*. This offers a technical advantage, as the structure of the original two-loop integrals can be simplified before integration, reducing the number of relevant scales down to a single scale, given by the ratio $\hat{s}/m_t^2$. The latter quantities are associated to the heavy scales in our approximation, leading to the hierarchy

$$p_T^2,\ m_Z^2 \ll \hat{s},\ m_t^2. \tag{6}$$

After the expansion and Integration-by-Parts (IBP) reduction, the box form factors are expressed as

$$\mathcal{A}_i^{(\square)} = \mathcal{N}(p_T^2, m_Z^2) \sum_{N=0}^{\infty} \sum_{i+j=N} c_{ij} (p_T^2)^i (m_Z^2)^j, \tag{7}$$

where the c_{ij} coefficients are linear combinations of the master integrals (MI) resulting from the IBP reduction, which in turn depend on $\hat{s}/m_t^2$, while $\mathcal{N}(p_T^2, m_Z^2)$ is an overall normalization factor which may depend on p_T^2 and m_Z^2. At NLO, we find a basis of 52 known MIs [27–32], two of which are elliptic integrals that can be evaluated using the routines of ref. [33].

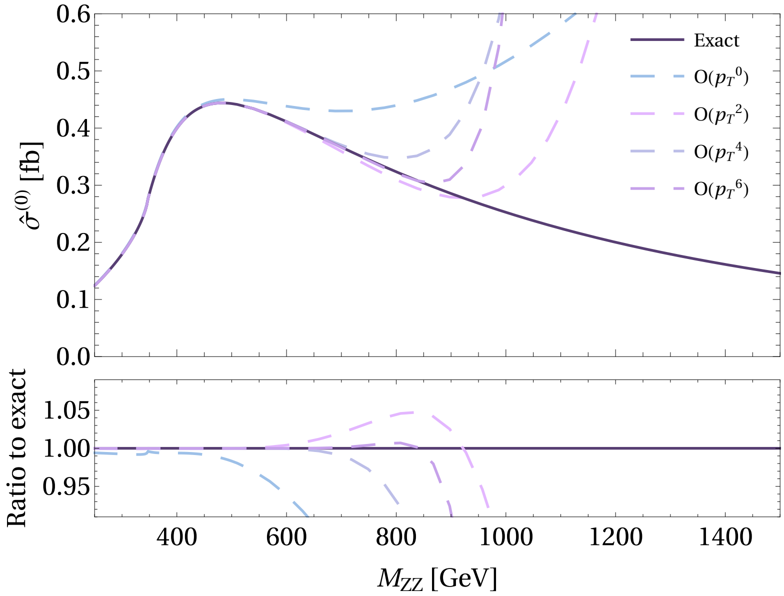

Figure 2: The partonic cross section at LO, $\hat{\sigma}^{(0)}$, including both triangle and box diagrams. The exact result is shown as a dark solid line, while the results obtained using different orders of the p_T expansion for the $\mathcal{A}_i^{(0,\square)}$ are shown as dashed lines. In the bottom part, the ratio of each order over the exact result is shown.

2.1 Merging the p_T and high-energy expansions

The p_T expansion can accurately reproduce the exact result only in a specific region of the physical phase space, corresponding to values $|\hat{t}| \lesssim 4m_t^2$ for any $\hat{s}$. For example, when looking at the partonic cross section at LO shown in fig. 2, one can see that the the accuracy is well below the percent level when the first few terms in the expansion are included, but the agreement is ensured only for $M_{ZZ} \lesssim 700$ GeV. Indeed, at higher invariant masses the region $|\hat{t}| \gtrsim 4m_t^2$ gives an increasingly important contribution to the box form factors, and the hierarchy of eq. (6) is not always justified. In ref. [23], it was shown that the correct behaviour of the amplitude at high energies can be accounted for by complementing the p_T expansion (or a similar forward expansion, see ref. [34]) with the HE expansion, which has been applied to $gg \to ZZ$ in ref. [20], assuming the scale hierarchy

$$m_Z^2 \ll m_t^2 \ll \hat{s}, \hat{t}. \tag{8}$$

Furthermore, to ensure that a good accuracy is maintained everywhere in phase space, it is important to improve the convergence of both expansions using Padé approximants. The results of this approach for the NLO form factor $\mathcal{A}_9^{(1,\square)}$ are shown in fig. 3. For a fixed value of $\hat{s}$, the border of validity of the p_T and HE expansions, where the solid lines show a divergent behaviour, is $-\hat{t}/(4m_t^2) \sim 1$. In the vicinity of this point, the Padé-improved versions of the p_T and HE expansion, shown as dashed lines, are well behaved, and they deviate with respect to each other by less than 0.1‰.

We implemented the Padé-improved form factors in analytic form into a FORTRAN code, which then uses the most suitable approximation for a given phase-space point. In particular, for the

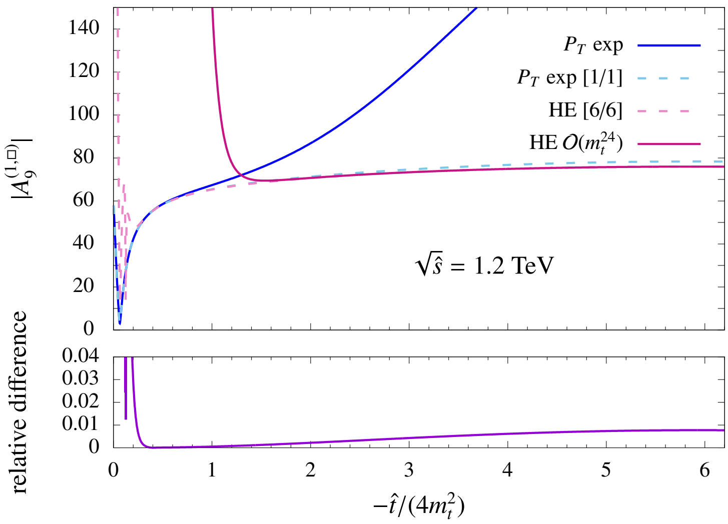

Figure 3: NLO form factor for $\sqrt{\hat{s}} = 1200$ GeV in various approximations: p_T expansion (solid blue), [1/1] Padé approximant based on the p_T expansion (dashed, light blue), high-energy expansion (solid, pink) and [6/6] HE Padé approximant (dashed, rosa). The lower panel shows the relative difference of the Padé approximants only.

high-energy region, defined by $|\hat{t}| > 4m_t^2$ and $|\hat{u}| > 4m_t^2$, we use a [6/6] Padé constructed from the HE expansion, while for the rest of the phase space we use a [1/1] Padé based on the p_T expansion.

We compared our results for the two-loop box diagrams with the helicity amplitudes obtained in the numerical calculation of ref. [13]. In fig. 4 we show the relative difference for the helicity amplitude ++00. We observe that, for both of the phase-space regions defined in our approach, the differences are below 1%, with the majority of phase-space points deviating by less than 0.1%.

3. Conclusions

We presented the computation of the top-mediated box diagrams for $gg \to ZZ$ at NLO in QCD using the p_T expansion, which provides accurate results in a phase-space region that so far has not been covered by other analytic approximations. Where a comparison with other approaches was possible, we found a very good agreement with previous calculations, both analytic and numerical. Furthermore, we have complemented our approximation with the results obtained in ref. [20], showing that a combination of the p_T and the HE expansions, improved using Padé approximants, allows a complete coverage of the phase space without a significant loss of accuracy. Since these results are in analytic form, they can be conveniently implemented in a Monte Carlo code for phenomenological studies.

A natural extension of this work would be to test the applicability of the p_T expansion to higher loops. Several steps in this direction have been taken in the case of a different $2 \to 2$ process, namely Higgs pair production. In this context, a complete account of the three-loop virtual corrections seems to require not only a forward expansion [35], but also asymptotic expansions [36].

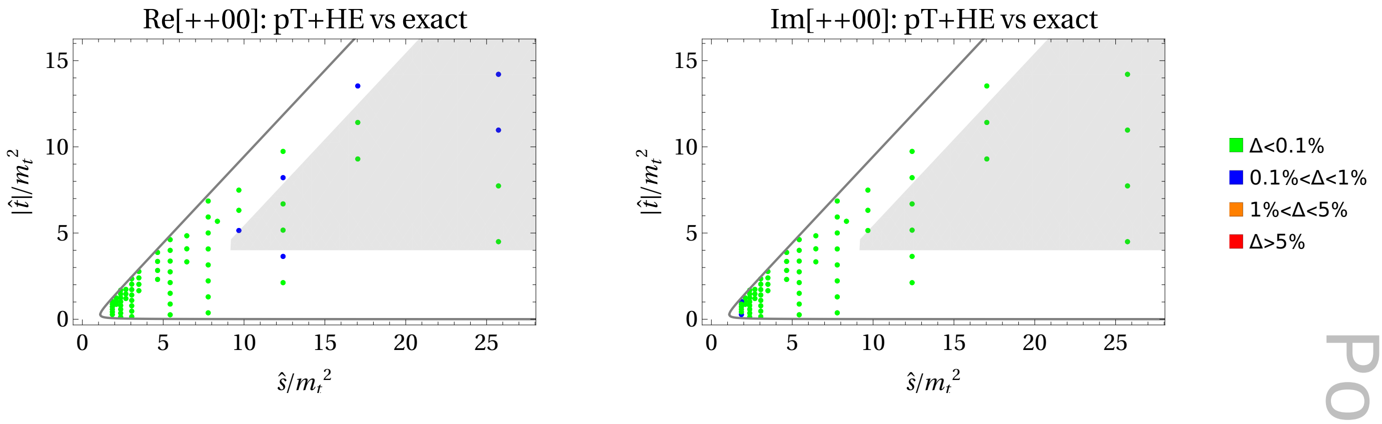

Figure 4: Relative difference between several phase-space points of ref. [13] and the merging of the Padé-improved p_T and HE expansions for the helicity amplitude ++00. Points in the shaded region are outside the formal limit of validity of the p_T expansion. The physical phase-space region is delimited by the grey line.

4. Acknowledgments

This work has been done in collaboration with Giusepe Degrassi and Ramona Gröber. We also thank Luigi Bellafronte and Pier Paolo Giardino for participating in the early stages of this project, and the authors of ref. [13] for providing us with the results for additional phase-space points and for useful discussions. We acknowledge support from the COMETA COST Action CA22130. This research was supported by the Deutsche Forschungsgemeinschaft (DFG, German Research Foundation) under grant 396021762 — TRR 257 "Particle Physics Phenomenology after the Higgs Discovery". The diagrams in this paper have been drawn using `JaxoDraw` [37].

References

[1] R.W. Brown and K.O. Mikaelian, *W^+W^- and Z^0Z^0 pair production in e^+e^-, pp, and $\overline{p}p$ colliding beams*, *Phys. Rev. D* **19** (1979) 922.

[2] J. Ohnemus and J.F. Owens, *Order-α_s calculation of hadronic zz production*, *Phys. Rev. D* **43** (1991) 3626.

[3] B. Mele, P. Nason and G. Ridolfi, *Qcd radiative corrections to z boson pair production in hadronic collisions*, *Nuclear Physics B* **357** (1991) 409.

[4] F. Cascioli, T. Gehrmann, M. Grazzini, S. Kallweit, P. Maierhöfer, A. von Manteuffel et al., *ZZ production at hadron colliders in NNLO QCD*, *Phys. Lett. B* **735** (2014) 311 [1405.2219].

[5] T. Gehrmann, A. von Manteuffel, L. Tancredi and E. Weihs, *The two-loop master integrals for $q\overline{q} \to VV$*, *JHEP* **06** (2014) 032 [1404.4853].

[6] F. Caola, J.M. Henn, K. Melnikov, A.V. Smirnov and V.A. Smirnov, *Two-loop helicity amplitudes for the production of two off-shell electroweak bosons in quark-antiquark collisions*, *JHEP* **11** (2014) 041 [1408.6409].

[7] T. Gehrmann, A. von Manteuffel and L. Tancredi, *The two-loop helicity amplitudes for $q\overline{q}' \to V_1 V_2 \to 4$ leptons*, JHEP **09** (2015) 128 [1503.04812].

[8] E. Accomando, A. Denner and A. Kaiser, *Logarithmic electroweak corrections to gauge-boson pair production at the LHC*, Nucl. Phys. B **706** (2005) 325 [hep-ph/0409247].

[9] A. Bierweiler, T. Kasprzik and J.H. Kühn, *Vector-boson pair production at the LHC to $O(\alpha^3)$ accuracy*, JHEP **12** (2013) 071 [1305.5402].

[10] J. Baglio, L.D. Ninh and M.M. Weber, *Massive gauge boson pair production at the LHC: a next-to-leading order story*, Phys. Rev. D **88** (2013) 113005 [1307.4331].

[11] D.A. Dicus, C. Kao and W.W. Repko, *Gluon production of gauge bosons*, Phys. Rev. D **36** (1987) 1570.

[12] E. Glover and J. Van der Bij, *Z-boson pair production via gluon fusion*, Nuclear Physics B **321** (1989) 561.

[13] B. Agarwal, S.P. Jones and A. von Manteuffel, *Two-loop helicity amplitudes for $gg \to ZZ$ with full top-quark mass effects*, JHEP **05** (2021) 256 [2011.15113].

[14] C. Brønnum-Hansen and C.-Y. Wang, *Top quark contribution to two-loop helicity amplitudes for Z boson pair production in gluon fusion*, JHEP **05** (2021) 244 [2101.12095].

[15] B. Agarwal, S. Jones, M. Kerner and A. von Manteuffel, *Complete NLO QCD Corrections to ZZ Production in Gluon Fusion*, 2404.05684.

[16] K. Melnikov and M. Dowling, *Production of two Z-bosons in gluon fusion in the heavy top quark approximation*, Phys. Lett. B **744** (2015) 43 [1503.01274].

[17] F. Caola, M. Dowling, K. Melnikov, R. Röntsch and L. Tancredi, *QCD corrections to vector boson pair production in gluon fusion including interference effects with off-shell Higgs at the LHC*, JHEP **07** (2016) 087 [1605.04610].

[18] J.M. Campbell, R.K. Ellis, M. Czakon and S. Kirchner, *Two loop correction to interference in $gg \to ZZ$*, JHEP **08** (2016) 011 [1605.01380].

[19] R. Gröber, A. Maier and T. Rauh, *Top quark mass effects in $gg \to ZZ$ at two loops and off-shell Higgs boson interference*, Phys. Rev. D **100** (2019) 114013 [1908.04061].

[20] J. Davies, G. Mishima, M. Steinhauser and D. Wellmann, *$gg \to ZZ$: analytic two-loop results for the low- and high-energy regions*, JHEP **04** (2020) 024 [2002.05558].

[21] R. Bonciani, G. Degrassi, P.P. Giardino and R. Gröber, *Analytical Method for Next-to-Leading-Order QCD Corrections to Double-Higgs Production*, Phys. Rev. Lett. **121** (2018) 162003 [1806.11564].

[22] L. Alasfar, G. Degrassi, P.P. Giardino, R. Gröber and M. Vitti, *Virtual corrections to $gg \to ZH$ via a transverse momentum expansion*, JHEP **05** (2021) 168 [2103.06225].

[23] L. Bellafronte, G. Degrassi, P.P. Giardino, R. Gröber and M. Vitti, *Gluon fusion production at NLO: merging the transverse momentum and the high-energy expansions*, JHEP **07** (2022) 069 [2202.12157].

[24] A. von Manteuffel and L. Tancredi, *The two-loop helicity amplitudes for $gg \to V_1V_2 \to 4$ leptons*, JHEP **06** (2015) 197 [1503.08835].

[25] F. Caola, J.M. Henn, K. Melnikov, A.V. Smirnov and V.A. Smirnov, *Two-loop helicity amplitudes for the production of two off-shell electroweak bosons in gluon fusion*, JHEP **06** (2015) 129 [1503.08759].

[26] G. Degrassi, R. Gröber and M. Vitti, *Virtual QCD corrections to $gg \to ZZ$: top-quark loops from a transverse-momentum expansion*, 2404.15113.

[27] U. Aglietti, R. Bonciani, G. Degrassi and A. Vicini, *Analytic Results for Virtual QCD Corrections to Higgs Production and Decay*, JHEP **01** (2007) 021 [hep-ph/0611266].

[28] R. Bonciani, P. Mastrolia and E. Remiddi, *Vertex diagrams for the QED form-factors at the two loop level*, Nucl. Phys. B **661** (2003) 289 [hep-ph/0301170].

[29] C. Anastasiou, S. Beerli, S. Bucherer, A. Daleo and Z. Kunszt, *Two-loop amplitudes and master integrals for the production of a Higgs boson via a massive quark and a scalar-quark loop*, JHEP **01** (2007) 082 [hep-ph/0611236].

[30] M. Becchetti and R. Bonciani, *Two-Loop Master Integrals for the Planar QCD Massive Corrections to Di-photon and Di-jet Hadro-production*, JHEP **01** (2018) 048 [1712.02537].

[31] S. Caron-Huot and J.M. Henn, *Iterative structure of finite loop integrals*, JHEP **06** (2014) 114 [1404.2922].

[32] A. von Manteuffel and L. Tancredi, *A non-planar two-loop three-point function beyond multiple polylogarithms*, JHEP **06** (2017) 127 [1701.05905].

[33] R. Bonciani, G. Degrassi, P.P. Giardino and R. Gröber, *A Numerical Routine for the Crossed Vertex Diagram with a Massive-Particle Loop*, Comput. Phys. Commun. **241** (2019) 122 [1812.02698].

[34] J. Davies, G. Mishima, K. Schönwald and M. Steinhauser, *Analytic approximations of $2 \to 2$ processes with massive internal particles*, JHEP **06** (2023) 063 [2302.01356].

[35] J. Davies, K. Schönwald and M. Steinhauser, *Towards $gg \to HH$ at next-to-next-to-leading order: Light-fermionic three-loop corrections*, Phys. Lett. B **845** (2023) 138146 [2307.04796].

[36] J. Davies, K. Schönwald, M. Steinhauser and M. Vitti, *Three-loop corrections to Higgs boson pair production: reducible contribution*, 2405.20372.

[37] D. Binosi and L. Theussl, *JaxoDraw: A Graphical user interface for drawing Feynman diagrams*, Comput. Phys. Commun. **161** (2004) 76 [hep-ph/0309015].

PoS(LL2024)040